Nanoscale 3-D (E, k_x, k_y) band structure imaging on graphene and intercalated graphene

A. A. Zakharov
C. Virojanadara
S. Watcharinyanon
R. Yakimova
L. I. Johansson

An x-ray photoemission electron microscope (X-PEEM) equipped with a hemispherical energy analyzer is capable of fast acquisition of momentum-resolved photoelectron angular distribution patterns in a complete cone. We have applied this technique to observe the 3-D (E, k_x, k_y) electronic band structure of zero-, one-, and two-monolayer (ML) graphene grown ex situ on 6H-SiC(0001) substrates where a carbon buffer layer (zero ML) forms underneath the graphene layer(s). We demonstrate that the interfacial buffer layer can be converted into quasi-free-standing graphene upon intercalation of Li atoms at the interface and that such a graphene is structurally and electronically decoupled from the SiC substrate. High energy and momentum resolution of the X-PEEM, along with short data acquisition times from submicrometer areas on the surface demonstrates the uniqueness and the versatility of the technique and broadens its impact and applicability within surface science and nanotechnology.

Introduction

Mapping of the electron band structure or the Fermi surface of a solid using angle-resolved photoelectron spectroscopy (ARPES) is commonly quite tedious and time consuming [1, 2]. The technique requires the mechanical scanning of the sample at least in one direction, and many photoelectron spectra typically have to be collected in order to fully determine the energy and the momentum of the electron states in the Brillouin zone. In this paper, we show that an energy-filtered x-ray photoemission electron microscope (X-PEEM) is capable of fast acquisition of momentum-resolved photoelectron angular distribution patterns. By imaging the diffraction plane of the objective lens [3], an energy slice of the photoelectron angular distribution pattern from a very small (<1 μm) area on the surface can be directly collected in a complete cone and projected on the screen. The microspectroscopy capability of the X-PEEM is well known; however, for the photoelectron angular distribution pattern from a nonhomogeneous sample, i.e., a sample with more than one stable phase on the surface, one has to be careful when acquiring data from different phases. The photoelectron angular distribution pattern is collected in a wide cone of angles. This means that no contrast aperture is used during the data acquisition, and photoelectrons from a much larger region [than that set by a selected area aperture (SAA)] on the surface may go through the optical system of the microscope (due to spherical aberration of the objective lens). To restrict the aberrations, we use an extremely small SAA and probe a submicrometer (800 nm) area of the sample. We first apply this technique to observe the 3-D (E, k_x, k_y) electronic band structure of zero-, one-, and two-monolayer (ML) graphene grown *ex situ* on 6H-SiC(0001) substrates where a carbon buffer layer (zero ML) forms underneath the graphene layer(s). In addition, we demonstrate that the interfacial buffer layer can be converted into a quasi-free-standing graphene upon intercalation of Li atoms.

The potential of graphene, i.e., a 2-D sheet of sp^2-bonded carbon atoms arranged in a honeycomb lattice, for advanced nanoelectronics applications has been abundantly demonstrated [4–6]. Among different methods of graphene preparation, the thermal decomposition of the SiC(0001) surface in ambient gas proved to be very successful to prepare large and homogeneous areas of single-layer

Digital Object Identifier: 10.1147/JRD.2011.2143570

©**Copyright** 2011 by International Business Machines Corporation. Copying in printed form for private use is permitted without payment of royalty provided that (1) each reproduction is done without alteration and (2) the Journal reference and IBM copyright notice are included on the first page. The title and abstract, but no other portions, of this paper may be copied by any means or distributed royalty free without further permission by computer-based and other information-service systems. Permission to republish any other portion of this paper must be obtained from the Editor.

0018-8646/11/$5.00 © 2011 IBM

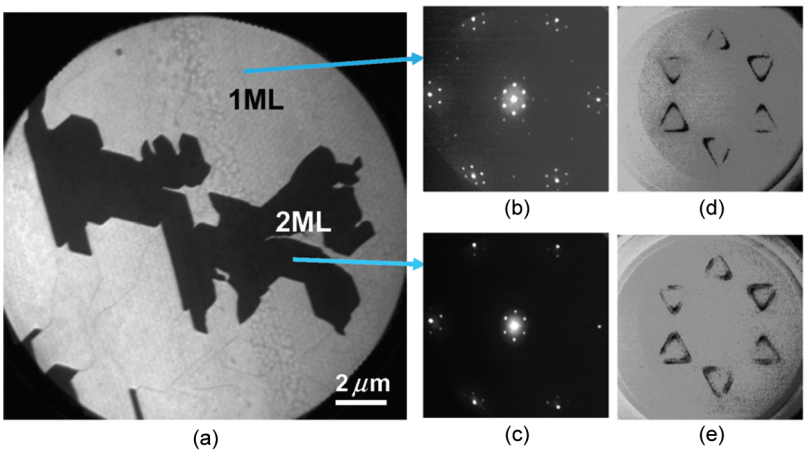

Figure 1

Low-energy electron microscope (LEEM) image (a) from an *ex situ* grown sample of one-monolayer (ML) graphene with two-ML islands; electron energy is 4.6 eV. Electron diffraction: μ-LEED images (400-nm sampling area) acquired at 60-eV electron energy from (b) one-ML and (c) two-ML areas. Photoelectron diffraction: high energy resolution 2-D (k_x, k_y) maps for (d) one-ML and (e) two-ML graphene taken at an electron binding energy of 2.5 eV below the Fermi level. Two π-bands are clearly seen from the two-ML island. The photon energy is 35 eV, and the energy resolution is set at 0.15 eV.

graphene on the SiC surface [7]. When epitaxial graphene layers are formed on SiC(0001), the first carbon layer (known as the "buffer" or "interfacial" layer) does not have the desirable electrical properties of graphene due to a disruption of the graphene π-bands by strong hybridization with the SiC substrate. The undesired effects originating from this strong coupling, such as intrinsic n-type doping and degraded transport properties, affect the overlying graphene layers. Most of the remaining problems regarding the graphene application are related to the presence of the buffer layer. It was shown [8–10] that quasi-free-standing epitaxial graphene can be obtained on SiC(0001) by hydrogen intercalation. In this paper, we demonstrate that the interfacial layer can be also converted into quasi-free-standing graphene upon the intercalation of Li atoms at the interface. The topmost Si atoms, which, for epitaxial graphene, are covalently bound to the buffer layer, are now saturated by lithium bonds. Evolution of the electronic band structure of the buffer layer during the intercalation process toward quasi-free-standing graphene was studied using an energy-filtered X-PEEM.

Experiment

Epitaxial graphene was grown on nominally on-axis 6H-SiC(0001) substrates in an inductively heated furnace under highly isothermal conditions at a temperature of 2,000 °C and at an ambient argon pressure of 1 atm [7]. The morphology, the thickness, and the electronic band structure of the graphene layers were investigated using a commercial low-energy electron microscope (LEEM; LEEM III, Elmitec GmbH) installed at the undulator beamline I311 of the synchrotron radiation facility MAX-lab in Lund. The linearly s-polarized radiation of the first harmonics of the undulator was used for the excitation, which is a normal incident to the sample surface (synchrotron light goes through the beam separator of the microscope). The energy filtering function is realized by utilizing a hemispherical analyzer in the electron optical path, and the lenses of the image column independently transfer the image plane and the back focal plane of the objective through the system. It is possible to switch between energy-filtered images of the surface and energy-filtered photoelectron emission angular distribution [3, 11–14]. A few MLs of Li were deposited *in situ* from a metal dispenser [Electrical Appliances and Scientific Society (SAES) Getters], and subsequent, annealing steps were carried out *live* in front of the objective lens. For the measurements presented here, the accelerating voltage of the microscope was 20 kV, and the projection optics was set to give a field of view of about ± 2 Å^{-1} in the momentum space; the settings readily cover the first and a part of the second Brillouin zone of graphene.

Results and discussion

To demonstrate the power of the X-PEEM for the fast acquisition of momentum-resolved photoelectron angular distribution patterns in a complete cone, we first collected data from a one-ML graphene sample with two-ML islands on it. **Figure 1(a)** shows a typical LEEM image from such a

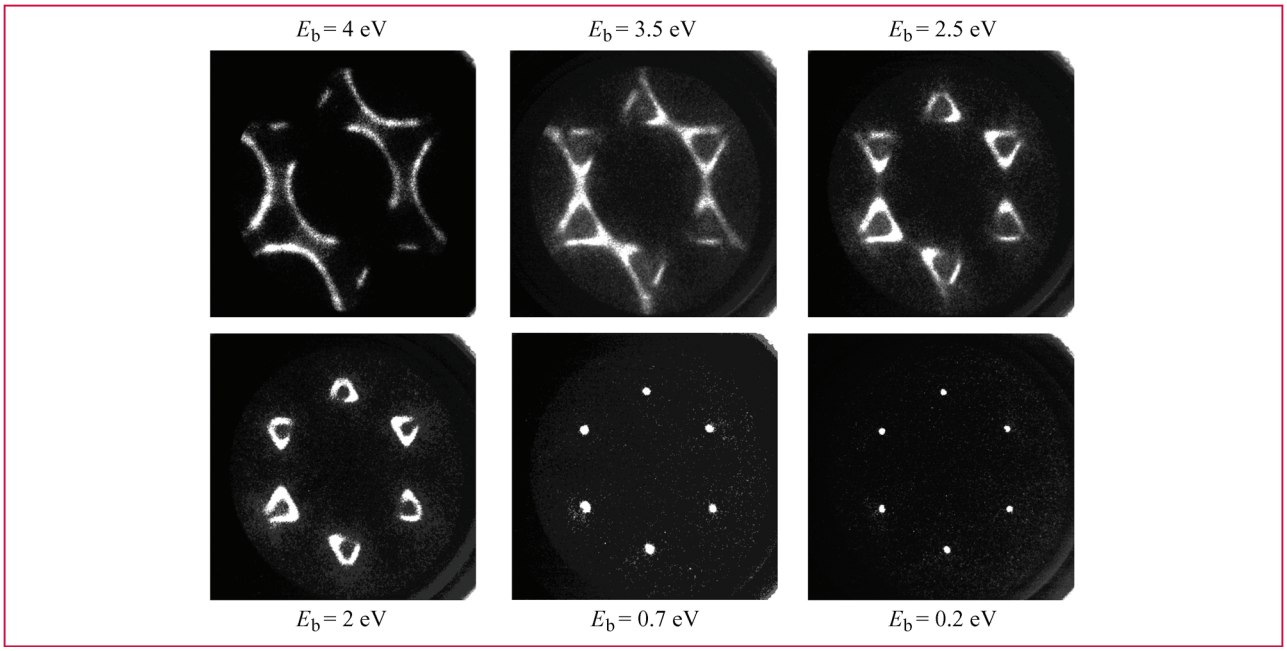

Figure 2

Energy-resolved 2-D (k_x, k_y) maps for one-ML graphene given by the angular distribution of photoelectrons acquired at a photon energy of 35 eV. The binding energy is indicated at each image. The images are collected from an area of 800-nm diameter on the surface. The energy resolution was set at 0.4 eV.

surface. The number of graphene layers can be immediately identified from the electron reflectivity curves (not shown), which demonstrate one minimum for one-ML area and two minima at the island areas. Based on earlier observation [7, 15] of the variation in the reflectivity with electron energy from graphene samples, one can conclude that islands in the LEEM image in Figure 1(a) correspond to two-ML graphene. Diffraction patterns [micro-low-energy electron diffraction (LEED)] originating from one- and two-ML areas [see **Figure 1(b)** and **1(c)**, respectively] show a distinct decrease in spot intensities around the main graphene spots for a two-ML island. Area-selected azimuthal distributions of the photoelectron intensity can be recorded by placing the SAA either on the one-ML surface or a two-ML island. In **Figure 1(d)** and **1(e)**, 2-D momentum-resolved photoelectron angular distribution patterns are shown at a 2.5-eV binding energy from a small (800 nm) area for one- and two-ML islands [see Figure 1(d) and (e), respectively]. For the two-ML island, the second π-band in the electronic band structure becomes clearly observable [see Figure 1(e)]. This demonstrates the microspectroscopy potential of the X-PEEM in photoelectron angular distribution mode when spherical aberrations of the objective lens are limited by using a small-enough sampling area on the surface. In **Figure 2**, 2-D (k_x, k_y) photoelectron angular distributions are shown as a function of electron energy down to 4 eV below the Fermi level. The shape of the well-known graphene band structure with the Dirac points approximately 0.4 eV below the Fermi level [16] is clearly reproduced in Figure 2. The binding energy in the bottom-right image is 0.2 eV above the Dirac point. The energy resolution for the energy scan was set to 0.4 eV, and the acquisition time of such a 2-D band structure map is quite short (about a minute per image, i.e., for one energy slice) compared with that of the usual ARPES. When higher energy resolution is needed, e.g., to resolve two π-bands for two-ML graphene [see Figure 1(e)], a smaller exit slit of the analyzer is used. The data set in Figure 1(e) was taken at an energy resolution of approximately 0.15 eV, and the image average acquisition time per image then increased up to several minutes. For the momentum resolution, an upper bound can be evaluated from extracted line profiles of the photoelectron intensity. The full width at half-maximum is estimated as 0.09 $Å^{-1}$ in momentum space at the 27-eV kinetic energy. Aside from the instrument resolution, the width has contributions from electron–phonon and electron–electron interactions.

Now, we turn to the problem of the buffer layer, which compromises the performance of the true graphene layer(s) grown on top of the buffer layer. It is known that the buffer layer can be lifted up and transferred to a free-standing graphene by exposing the surface to atomic hydrogen [8–10].

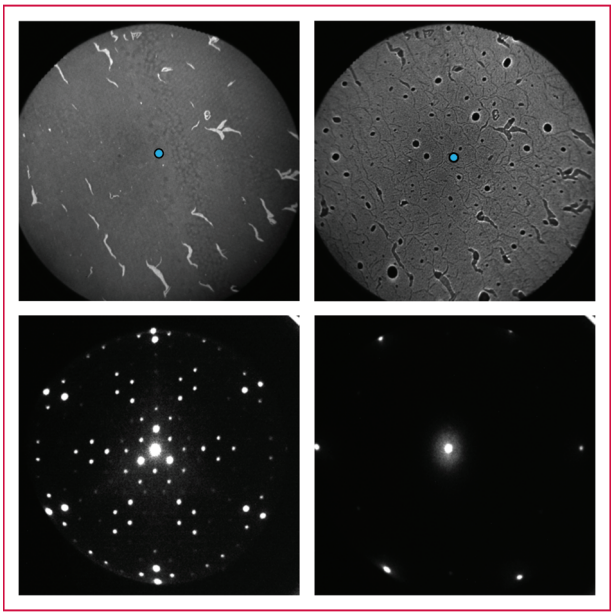

Figure 3

Mirror image of the zero-ML buffer layer surface (top left) before and (top right) after Li intercalation with the corresponding LEED patterns collected from the circular marked area in the center of the images. Electron energy is +0.5 eV for the pristine buffer layer mirror image and −1.6 eV for the intercalated one. The much lower electron energy after intercalation is due to the change in the work function of the Li-covered surface. The electron energies for the corresponding LEED pattern are 30 and 40 eV before and after intercalation, respectively.

Recently, electronic decoupling of an epitaxial graphene has been also demonstrated by gold intercalation [17]. There were speculations that hydrogen saturates Si bonds and decouples the buffer layer from the substrate since it is not possible to detect hydrogen in photoelectron spectroscopy. In this paper, we used Li metal for intercalation to have full control over the intercalation process due to the readily detectable Li 1s core level [18]. The sample for this paper was the pristine buffer layer graphene that turned into a quasi-free-standing graphene layer after Li intercalation. This sample was prepared under conditions similar to those used in the sample shown in Figure 1 but annealed for a shorter time. In **Figure 3**, mirror-mode micrographs, along with micro-LEED patterns, are shown in the same area of the sample without (top row) and with (bottom row) intercalated lithium. One can see that the pristine surface before intercalation contains small stripes of one-ML graphene (white areas in the top-left image) and is thus not homogeneous. The contrast in the image is due to different reflectivity of zero- and one-ML areas at the chosen electron energy. After lithium treatment, the surface becomes even more nonhomogeneous due to the formation of Li droplets (black dots in the top-right image). This demonstrates the advantage and need to use a real microscopy technique to reveal the electronic band structure of the intercalated buffer layer. The contrast in the top-right image has markedly changed due to the formation of a dipole layer at the surface/interface region, originating from the electron doping of graphene after Li intercalation [18]. This is manifested by a 2-eV lower electron energy used for the top-right mirror image and a 2-eV shift of the C1s and Si2p bulk SiC photoelectron peaks (not shown). For the pristine buffer layer, the LEED pattern shows intense superstructure spots (bottom-left image) due to the covalent bonding to the SiC substrate. After lithium treatment, the superstructure spots are barely seen (bottom-right image), which suggests the absence or the weakening of the interlayer bonding. This is already an evidence of a geometrical decoupling of the interface layer from the substrate. Aside from these structural aspects, the lithium treatment has a dramatic effect on the electronic structure of the intercalated samples. Most obviously, it is demonstrated by measured momentum-resolved photoelectron angular distribution patterns before and after intercalation. The angular distribution patterns were collected from the same marked area in the upper row of Figure 3 far enough away from one-ML stripes and Li droplets. In **Figure 4**, such a comparison is made for four chosen electron energies. For a pristine zero layer, only very faint delocalized and smeared-out states can be seen below the 1-eV binding energy, and no π-bands are visible close to the Fermi level. However, after lithium treatment, the linear dispersing π-bands of ML graphene appear. The energy resolution for this band mapping was set to 0.4 eV, but the angular distribution pattern for energies close to the Fermi level [Figure 4, bottom row, rightmost image] displays quite sharp energy bands, which are much sharper than the symmetrical structure 1 eV below the Dirac points [see Figure 4, bottom row, second image]. The reason for this is that, when going from occupied to unoccupied states at the Fermi wave vector, one will get a sharp cutoff given by the Fermi function that is much narrower than the analyzer resolution. Thus, the band mapping of the Fermi surfaces can be conducted at higher energy resolution than set by the energy analyzer. Figure 4 clearly shows that, after intercalation, quasi-free-standing one-ML graphene is strongly n-doped since the Dirac points move away from the Fermi level by approximately 1 eV. Based on the linear dispersion of the density of states near the Dirac point [19], the electron carrier concentration of doped graphene can be estimated using the following equation:

$$N_e = \frac{(E_f - E_d)^2}{\pi (hV_f)^2},$$

where N_e is the electron areal density, $V_f \approx 10^6$ m/s is the Fermi velocity of graphene, h is Planck's constant, E_f and

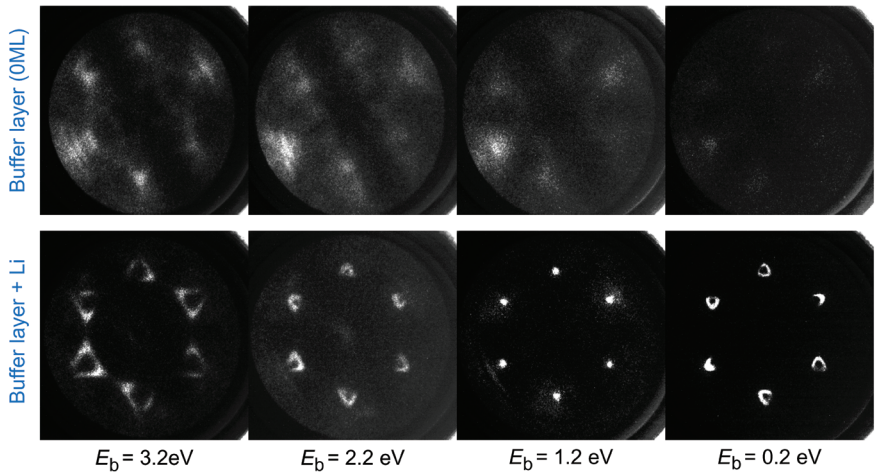

Figure 4

Two-dimensional (k_x, k_y) maps for the zero-monolayer (ML) buffer layer (upper row) and the Li-intercalated buffer layer (bottom row) at several binding energies. The photon energy is 35 eV. The π-bands are absent in the pristine zero-ML sample but are clearly seen after Li intercalation and now with the Dirac points approximately 1 eV below the Fermi level.

E_d are the energy position of the Fermi level and the Dirac point, respectively. After lithium deposition and intercalation, the n-type doping of the free-standing graphene shifts the graphene band down by approximately 1 eV with respect to the Fermi level, and hence, E_f moves to 1.2 eV above the Dirac point [see Figure 4, bottom row, third image]. From the aforementioned equation, the electron density is estimated to be around 1.0×10^{14} cm^{-2}, suggesting the effective electron doping of free-standing graphene by lithium electrons.

Summary

In this paper, we have demonstrated that the energy-filtered X-PEEM is capable of the fast acquisition of momentum-resolved photoelectron angular distribution patterns in a complete cone from submicrometer areas on the surface. We have applied this technique to observe the 3-D (E, k_x, k_y) electronic band structure of zero-, one-, and two-ML graphene grown *ex situ* on 6H-SiC(0001) substrates that have a carbon buffer layer (zero ML) underneath the graphene layer(s). We have shown that the distinct differences in the π-band structure for a different number of graphene layers are clearly reflected in recorded angular distribution patterns. The technique has been thus shown to work for a nonhomogeneous sample, i.e., a sample having more than one stable phase on the surface, when a small-enough sampling area is probed to limit the spherical aberrations of the objective lens. We have also demonstrated that the buffer layer is turned into a quasi-free-standing graphene layer by lithium intercalation. The lithium passivates the underlying topmost Si atoms, donates electrons to the graphene layer, and produces a dramatic change in the electronic structure. The appearance of the typical linear π-bands during intercalation has been followed using the X-PEEM. The results presented demonstrate the uniqueness and the versatility of high-energy and momentum-resolved X-PEEM and broaden the applicability and the impact of this technique within surface science and nanotechnology.

Acknowledgments

This work was supported by the Swedish National Energy Administration.

References

1. A. Damascelli, “Probing the electronic structure of complex systems by ARPES,” *Phys. Script.*, vol. T109, pp. 61–74, 2004.
2. Z.-X. Shen and D. S. Dessau, “Electronic structure and photoemission studies of late transition-metal oxides–Mott insulators and high-temperature superconductors,” *Phys. Rep.*, vol. 253, no. 1–3, pp. 1–162, Mar. 1995.
3. T. Schmidt, S. Heun, J. Slezak, J. Diaz, K. C. Prince, G. Lilienkamp, and E. Bauer, “SPELEEM: Combining LEEM and spectroscopic imaging,” *Surf. Rev. Lett.*, vol. 5, no. 6, pp. 1287–1296, 1998.
4. C. Berger, Z. Song, X. Li, X. Wu, N. Brown, C. Naud, D. Mayou, T. Li, J. Haas, A. N. Marchenkov, E. H. Conrad, P. N. First, and W. A. de Heer, “Electronic confinement and coherence in patterned epitaxial graphene,” *Science*, vol. 312, no. 5777, pp. 1191–1196, May 2006.
5. T. Seyller, A. Bostwick, K. V. Emtsev, K. Horn, L. Ley, L. McChesney, T. Ohta, J. D. Riley, E. Rotenberg, and F. Speck, “Epitaxial graphene: A new material,” *Phys. Stat. Sol. (B)*, vol. 245, no. 7, pp. 1436–1446, Jul. 2008.

6. Y.-M. Lin, C. Dimitrakopoulos, K. A. Jenkins, D. B. Farmer, H.-Y. Chiu, A. Grill, and P. Avouris, "100-GHz transistors from wafer-scale epitaxial graphene," *Science*, vol. 327, no. 5966, pp. 662, Feb. 2010.
7. C. Virojanadara, M. Syvajarvi, R. Yakimova, L. I. Johansson, A. A. Zakharov, and T. Balasubramanian, "Homogeneous large-area graphene layer growth on 6H-SiC(0001)," *Phys. Rev. B*, vol. 78, no. 24, pp. 245403-1–245403-6, Dec. 2008.
8. C. Riedl, C. Coletti, T. Iwasaki, A. A. Zakharov, and U. Starke, "Quasi-free-standing epitaxial graphene on SiC obtained by hydrogen intercalation," *Phys. Rev. Lett.*, vol. 103, no. 24, pp. 246804-1–246804-4, Dec. 2009.
9. C. Virojanadara, A. A. Zakharov, R. Yakimova, and L. I. Johansson, "Buffer layer free large area bi-layer graphene on SiC(0001)," *Surf. Sci. Lett.*, vol. 604, pp. L4–L7, 2010.
10. F. Speck, M. Ostler, J. Röhrl, J. Jobst, D. Waldmann, M. Hundhausen, L. Ley, H. B. Weber, and T. Seyller, "Quasi-freestanding graphene on SiC(0001)," *Mater. Sci. Forum*, vol. 645–648, pp. 629–632, 2010.
11. R. M. Tromp, Y. Fujikawa, J. B. Hannon, A. W. Ellis, A. Berghaus, and O. Schaff, "A simple energy filter for low energy electron microscopy/photoelectron emission microscopy instruments," *J. Phys., Condens. Matter*, vol. 21, no. 31, pp. 314007-1–314007-13, Aug. 2009.
12. P. Sutter, M. S. Hybertsen, J. T. Sadowski, and E. Sutter, "Electronic structure of few-layer epitaxial graphene on Ru(0001)," *Nano Lett.*, vol. 9, no. 7, pp. 2654–2660, Jul. 2009.
13. E. Sutter, D. P. Acharya, J. T. Sadowski, and P. Sutter, "Scanning tunneling microscopy on epitaxial bilayer graphene on ruthenium (0001)," *Appl. Phys. Lett.*, vol. 94, no. 13, pp. 133101-1–133101-3, Mar. 2009.
14. P. Sutter, J. T. Sadowski, and E. Sutter, "Graphene on Pt(111): Growth and substrate intercalation," *Phys. Rev. B*, vol. 80, no. 24, pp. 245411-1–245411-10, Dec. 2009.
15. H. Hibino, H. Kageshima, F. Maeda, M. Nagase, Y. Kobayashi, and H. Yamaguchi, "Microscopic thickness determination of thin graphite films formed on SiC from quantized oscillation in reflectivity of low energy electrons," *Phys. Rev. B*, vol. 77, no. 7, pp. 075413-1–075413-7, Feb. 2008.
16. T. Ohta, A. Bostwick, J. L. McChesney, T. Seyller, K. Horn, and E. Rotenberg, "Interlayer interaction and electronic screening in multilayer graphene investigated with angle-resolved photoemission spectroscopy," *Phys. Rev. Lett.*, vol. 98, no. 20, pp. 206802-1–206802-4, May 2007.
17. I. Gierz, T. Suzuki, R. T. Weitz, D. S. Lee, B. Krauss, C. Riedl, U. Starke, H. Höchst, J. H. Smet, C. R. Ast, and K. Kern, "Electronic decoupling of an epitaxial graphene monolayer by gold intercalation," *Phys. Rev. B*, vol. 81, no. 23, pp. 235408-1–235408-6, Jun. 2010.
18. C. Virojanadara, S. Watcharinyanon, A. A. Zakharov, and L. I. Johansson, "Epitaxial graphene on 6H-SiC and Li intercalation," *Phys. Rev. B*, vol. 82, no. 20, pp. 205402-1–205402-6, Nov. 2010.
19. A. H. Castro Neto, F. Guinea, N. M. R. Peres, K. S. Novoselov, and A. K. Geim, "The electronic properties of graphene," *Rev. Mod. Phys.*, vol. 81, no. 1, pp. 109–162, Jan.–Mar. 2009.

Received September 12, 2010; accepted for publication February 1, 2011

Alexei Alexeevich Zakharov *MAX-lab, Lund University, S-22100, Lund, Sweden (Alexei.Zakharov@maxlab.lu.se).*

Chariya Virojanadara *Department of Physics, Chemistry and Biology, Linköping University, S-58183, Linköping, Sweden (chavi@ifm.liu.se).*

Somsakul Watcharinyanon *Department of Physics, Chemistry and Biology, Linköping University, S-58183, Linköping, Sweden (somwat@ifm.liu.se).*

Rositza Yakimova *Department of Physics, Chemistry and Biology, Linköping University, S-58183, Linköping, Sweden (roy@ifm.liu.se).*

Leif Ingemar Johansson *Department of Physics, Chemistry and Biology, Linköping University, S-58183, Linköping, Sweden (lejoh@ifm.liu.se).*